International Journal of Fracture Fatigue and Wear, Volume 4

Proceedings of the 5th International Conference on
Fracture Fatigue and Wear, pp. 70-77, 2016

NONLINEAR CONTROL OF SMART PLATES USING ISOGEOMETRIC ANALYSIS

P. Phung-Van[1,2], Loc V. Tran[1,2], H. Nguyen-Xuan[3] and M. Abdel-Wahab[1,2]

[1]Division of Computational Mechanics, Ton Duc Thang University, Vietnam

[2]Faculty of Engineering and Architecture, Ghent University, Belgium

[3]Center for Interdisciplinary Research in Technology, HUTECH University, Vietnam

Abstract: In this paper, isogeometric analysis (IGA) based on a generalized unconstrained approach for nonlinear analysis of smart composite plates is investigated. In composite plates, the mechanical displacement field is approximated according to the proposal model and the nonlinear formulation for plates is based on the von Kármán strains. Through the thickness of each piezoelectric layer, the electric potential is assumed linearly. For active control of the piezoelectric composite plates, a close-loop system is used. Various numerical examples are investigated to show high accuracy and reliability of the proposed method.

Keywords: Nonlinear control, isogeometric analysis (IGA), smart materials, piezoelectric plates.

1. INTRODUCTION

Piezoelectric materials belong to a smart material class that expresses electromechanical coupling. The main feature of smart materials is transformation between mechanical energy and electric energy. When the application of electric field to piezoelectric structures is considered, the mechanical deformation is generated. With the advantages of piezoelectric materials, various numerical methods have been devised. Mitchell and Reddy [1] presented the classical plate theory (CPT) using the third order shear deformation theory (TSDT) to obtain the Navier solution for composite laminates with piezoelectric lamina. The radial point interpolation method (RPIM) combined with the first order shear deformation theory (FSDT) and the CPT with rectangular plate bending element were investigated by Liu et al. [2] to compute and simulate the static deformation and responses of smart plates. A HSDT-layerwise generalized finite element formulation [3] and the layerwise based on analytical formulation [4] were investigated to study piezoelectric composite plates. For vibration control, Bailey et al [5] and Shen et al. [6] investigated smart beams integrated with layers using analytical solutions. Wang et al. [7] used FEM to investigate dynamic stability of piezoelectric composite plates, where the governing equations of motion using Lyapunov's energy with active damping was used. Recently, isogeometric analysis (IGA) has been developed to investigate the piezoelectric composite plates [8] and plates/shells [9-13]. However, nonlinear transient analysis has not considered in their previous work. Hence, this paper tries to fill this gap by using IGA based on the general unconstrained third order shear deformation theory (UTSDT). For reference, it is termed as IGA-UHSDT. The method will be applied for nonlinear analysis of piezoelectric composite plates. The IGA-UHSDT is used to approximate the displacement field of smart plates. Through the thickness of each piezoelectric layer, the electric potential is assumed linearly. The nonlinear formulation for plates is formed in the total Lagrange approach based on the von Kármán strains. The reliability and accuracy of the method are confirmed by numerical examples.

2. FORMULATION OF PIEZOELECTRICITY

Consider a piezoelectric composite plate as shown in Figure 1, the lower and upper layers of the composite plate are piezoelectric layers. The UHSDT is used to approximate the variable displacements for the composite plate, while the electrical displacements are assumed to be independent.

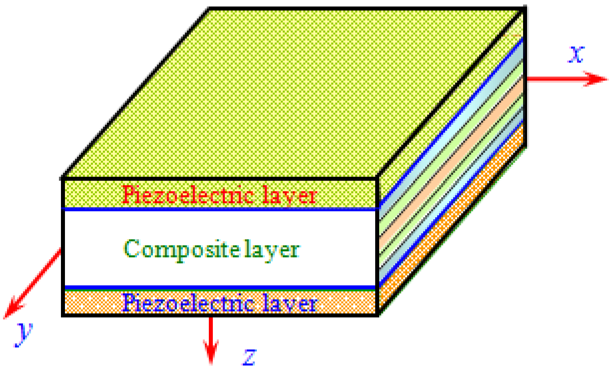

Fig. 1 Configuration of a piezoelectric laminated composite plate.

2.1. UHSDT

The unconstrained theory based on HSDT can be rewritten

$$\begin{aligned} u(x,y,z,t) &= u_0(x,y,t) + z u_1(x,y,t) + f(z) u_2(x,y,t) \\ v(x,y,z,t) &= v_0(x,y,t) + z v_1(x,y,t) + f(z) v_2(x,y,t) \\ w(x,y,z,t) &= w(x,y,t) \end{aligned} \quad (1)$$

where u_0, u_1, u_2, v_0, v_1, v_2 and w are displacement variables. For UTSDT in [14], the function $f(z) = z^3$ is used. In what follows, we introduce a new function $f(z) = arctan(z)$ that ensures that its first derivative is nonlinear through the plate thickness and solutions are more accurate than for the case of $f(z) = z^3$.

For a plate bending, the strain vector is represented by:

$$\varepsilon_{ij} = \frac{1}{2}\left(\frac{\partial u_i}{\partial x_j} + \frac{\partial u_j}{\partial x_i}\right) + \frac{1}{2}\frac{\partial u_k}{\partial x_i}\frac{\partial u_k}{\partial x_j} \quad (2)$$

The material behavior of smart composite plates is expressed as follows [15]:

$$\begin{bmatrix} \boldsymbol{\sigma} \\ \mathbf{D} \end{bmatrix} = \begin{bmatrix} \mathbf{c} & -\mathbf{e}^T \\ \mathbf{e} & \mathbf{g} \end{bmatrix} \begin{bmatrix} \bar{\boldsymbol{\varepsilon}} \\ \mathbf{E} \end{bmatrix} \quad (3)$$

where $\bar{\boldsymbol{\varepsilon}}$ and $\boldsymbol{\sigma}$ are the strain vector and the stress vector, respectively; **g** denotes the dielectric constant matrix and **D** is the dielectric displacement; **e** is the piezoelectric constant; **E**, the electric field vector, can be defined as:

$$\mathbf{E} = -\text{grad}\phi \quad (4)$$

in which ϕ is the electric potential field; and **c**, the elasticity matrix, is defined as:

$$\mathbf{c} = \begin{bmatrix} \mathbf{A} & \mathbf{B} & \mathbf{L} & \mathbf{0} & \mathbf{0} \\ \mathbf{B} & \mathbf{G} & \mathbf{F} & \mathbf{0} & \mathbf{0} \\ \mathbf{L} & \mathbf{F} & \mathbf{H} & \mathbf{0} & \mathbf{0} \\ \mathbf{0} & \mathbf{0} & \mathbf{0} & \mathbf{A}_s & \mathbf{B}_s \\ \mathbf{0} & \mathbf{0} & \mathbf{0} & \mathbf{B}_s & \mathbf{D}_s \end{bmatrix}; \mathbf{e}^{(k)} = \begin{bmatrix} 0 & 0 & 0 & 0 & d_{15} & 0 \\ 0 & 0 & 0 & d_{15} & 0 & 0 \\ d_{31} & d_{32} & d_{33} & 0 & 0 & 0 \end{bmatrix}^{(k)}; \mathbf{g}^{(k)} = \begin{bmatrix} p_{11} & 0 & 0 \\ 0 & p_{22} & 0 \\ 0 & 0 & p_{33} \end{bmatrix}^{(k)} \quad (5)$$

in which:

$$\begin{aligned} (\mathbf{A}, \mathbf{B}, \mathbf{G}, \mathbf{L}, \mathbf{F}, \mathbf{H}) &= \int_{-h/2}^{h/2} \left(1, z, z^2, f(z), zf(z), f^2(z)\right) \bar{Q}_{ij} \mathrm{d}z \qquad i, j = 1, 2, 6 \\ (\mathbf{A}_s, \mathbf{B}_s, \mathbf{D}_s) &= \int_{-h/2}^{h/2} \left(1, f'(z), \left(f'(z)\right)^2\right) \bar{Q}_{ij} \mathrm{d}z \qquad i, j = 4, 5 \end{aligned} \quad (6)$$

where $\bar{Q}_{ij}$ is calculated as in [1].

2.2. The piezoelectric plate formulation based on NURBS basic functions

2.2.1. Mechanical displacement

Using NURBS basic function, the field **u** of the composite plate is approximated as:

$$\mathbf{u}^h(\xi, \eta) = \sum_{I=1}^{m \times n} N_I(\xi, \eta) \mathbf{d}_I \quad (7)$$

where $\mathbf{d}_I = \begin{bmatrix} u_{0I} & v_{0I} & u_{1I} & v_{1I} & u_{2I} & v_{2I} & w_I \end{bmatrix}^T$, and N_I is the shape function as defined in [16].

The strains can be rewritten as:

$$\bar{\boldsymbol{\varepsilon}} = [\boldsymbol{\varepsilon}_p \quad \boldsymbol{\varepsilon}_s]^T = \sum_{I=1}^{m \times n} \left(\mathbf{B}_I^L + \frac{1}{2} \mathbf{B}_I^{NL} \right) \mathbf{d}_I \quad (8)$$

where $\mathbf{B}_I^L = \begin{bmatrix} \mathbf{B}_I^0 & \mathbf{B}_I^1 & \mathbf{B}_I^2 & \mathbf{B}_I^{s0} & \mathbf{B}_I^{s1} \end{bmatrix}^T$, in which

$$\mathbf{B}_I^{s0} = \begin{bmatrix} 0 & 0 & N_I & 0 & 0 & 0 & N_{I,x} \\ 0 & 0 & 0 & N_I & 0 & 0 & N_{I,y} \end{bmatrix}, \quad \mathbf{B}_I^{s1} = \begin{bmatrix} 0 & 0 & 0 & 0 & N_I & 0 & 0 \\ 0 & 0 & 0 & 0 & 0 & N_I & 0 \end{bmatrix}$$

$$\mathbf{B}_I^{2} = \begin{bmatrix} 0 & 0 & 0 & 0 & N_{I,x} & 0 & 0 \\ 0 & 0 & 0 & 0 & 0 & N_{I,y} & 0 \\ 0 & 0 & 0 & 0 & N_{I,y} & N_{I,x} & 0 \end{bmatrix}, \quad \mathbf{B}_I^{NL}(\mathbf{d}) = \begin{bmatrix} w_{I,x} & 0 \\ 0 & w_{I,y} \\ w_{I,y} & w_{I,x} \end{bmatrix} \begin{bmatrix} 0 & 0 & 0 & 0 & 0 & 0 & N_{I,x} \\ 0 & 0 & 0 & 0 & 0 & 0 & N_{I,x} \end{bmatrix} = \mathbf{A}_\theta \mathbf{B}_I^g \tag{9}$$

$$\mathbf{B}_I^{0} = \begin{bmatrix} N_{I,x} & 0 & 0 & 0 & 0 & 0 & 0 \\ 0 & N_{I,y} & 0 & 0 & 0 & 0 & 0 \\ N_{I,y} & N_{I,x} & 0 & 0 & 0 & 0 & 0 \end{bmatrix}, \quad \mathbf{B}_I^{1} = \begin{bmatrix} 0 & 0 & N_{I,x} & 0 & 0 & 0 & 0 \\ 0 & 0 & 0 & N_{I,y} & 0 & 0 & 0 \\ 0 & 0 & N_{I,y} & N_{I,x} & 0 & 0 & 0 \end{bmatrix},$$

2.2.2. Electric potential field

The electric potential field is approximated as follows [15]:

$$\phi^i(z) = \mathbf{N}_\phi^i \boldsymbol{\phi}^i \tag{10}$$

where $\mathbf{N}_\phi^i$ is the shape functions

The electric field **E** in Eq. (4) can be rewritten:

$$\mathbf{E} = -\nabla \mathbf{R}_\phi^i \boldsymbol{\phi}^i = -\mathbf{B}_\phi \boldsymbol{\phi}^i \tag{11}$$

2.2.3. Governing equations

The equations for the smart plate are written as:

$$\begin{bmatrix} \mathbf{M}_{uu} & 0 \\ 0 & 0 \end{bmatrix} \begin{bmatrix} \ddot{\ldots} \\ \ddot{\boldsymbol{\phi}} \end{bmatrix} \ldots \begin{bmatrix} \cdot_{uu} & \mathbf{K}_{u\phi} \\ \cdot_{\phi u} & \mathbf{K}_{\phi\phi} \end{bmatrix} \begin{bmatrix} \mathbf{d} \\ \boldsymbol{\phi} \end{bmatrix} = \begin{bmatrix} \mathbf{f} \\ \mathbf{Q} \end{bmatrix} \Leftrightarrow \bar{\mathbf{M}}\ddot{\ldots} = \bar{\mathbf{f}} \tag{12}$$

and for dynamic control

$$\mathbf{M}\ddot{\ldots} = \mathbf{F} \tag{13}$$

where $\mathbf{K}^* = \mathbf{K}_{uu} + G_d \left[\mathbf{K}_{u\phi}\right]_s \left[\mathbf{K}_{\phi\phi}^{-1}\right]_s \left[\mathbf{K}_{\phi u}\right]_s$ in which where G_d is the constant gains of the displacement feedback control, and

$$\begin{aligned} &\mathbf{K}_{uu} = \int_\Omega (\mathbf{B}^L + \mathbf{B}^{NL})^T \mathbf{c} (\mathbf{B}^L + \tfrac{1}{2}\mathbf{B}^{NL}) \mathrm{d}\Omega \quad ; \quad \mathbf{K}_{u\phi} = \int_\Omega (\mathbf{B}^L)^T \mathbf{e}^T \mathbf{B}_\phi \mathrm{d}\Omega \\ &\mathbf{K}_{\phi\phi} = \int_\Omega \mathbf{B}_\phi^T \mathbf{p} \mathbf{B}_\phi \mathrm{d}\Omega \quad ; \quad \mathbf{M}_{uu} = \int_\Omega \tilde{\ldots} \ldots \tilde{\ldots} \quad , \quad \mathbf{f} = \int_\Omega \bar{q}_0 \bar{\mathbf{N}} \mathrm{d}\Omega \end{aligned} \tag{14}$$

in which q_0 is a uniform load; $\bar{\mathbf{N}} = \begin{bmatrix} 0 & 0 & 0 & 0 & 0 & 0 & N_I \end{bmatrix}$; **m** is defined by:

$$\mathbf{m} = \begin{bmatrix} I_1 & I_2 & I_4 \\ I_2 & I_3 & I_5 \\ I_4 & I_5 & I_7 \end{bmatrix}, \quad (I_1, I_2, I_3, I_4, I_5, I_7) = \int_{-h/2}^{h/2} \rho \left(1, z, z^2, f(z), zf(z), f^2(z)\right) \mathrm{d}z \tag{15}$$

and

$$\tilde{\mathbf{N}} = \begin{Bmatrix} \mathbf{N}_1 \\ \mathbf{N}_2 \\ \mathbf{N}_3 \end{Bmatrix}, \ \mathbf{N}_1 = \begin{bmatrix} N_I & 0 & 0000 & 0 \\ 0 & N_I & 0000 & 0 \\ 0 & 0 & 0000 & N_I \end{bmatrix}, \mathbf{N}_2 = \begin{bmatrix} 00 & N_I & 0 & 000 \\ 00 & 0 & N_I & 000 \\ 0 & 0 & 0 & 000 \end{bmatrix}, \mathbf{N}_3 = \begin{bmatrix} 00000 & N_I & 0 \\ 00000 & 0 & N_I \\ 00000 & 0 & 0 \end{bmatrix} \tag{16}$$

3. NUMERICAL RESULTS

3.1. Static analysis

A square smart plate with length 20 cm under a uniform load q = 100 N/m^2 is considered. The plate has six layers: two outer piezo layers represented by *pie* and four composite layers. Each layer thickness of the non-piezoelectric composite plate is 0.25 mm and the thickness of the piezo layer is 0.1 mm. The composite layers are made of T300/976 graphite/epoxy and the piezo-ceramic layers are PZTG1195N. First, the effect of input voltages on deflection of the CFFF plate [*pie*/-45/45]$_{as}$ is shown in Figure 2a. It can be seen, the present results agree well with those of Liu et al. (2004). Furthermore, the deflection of the plate using only mesh of 9×9 elements with different boundary conditions (CFFF, SSFF, SSSS) is shown in Figure 2b. Again, it can be seen that the present method agrees very well with those of RPIM [2].

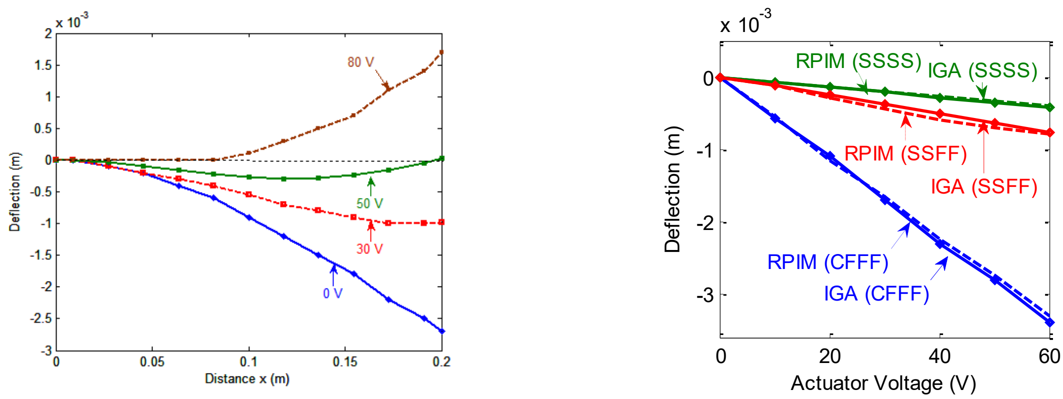

(a) (b)

Fig. 2 (a) Effect of input voltages on deflection of the piezoelectric composite plate; (b) The deflection of the piezoelectric composite plates with various boundary conditions

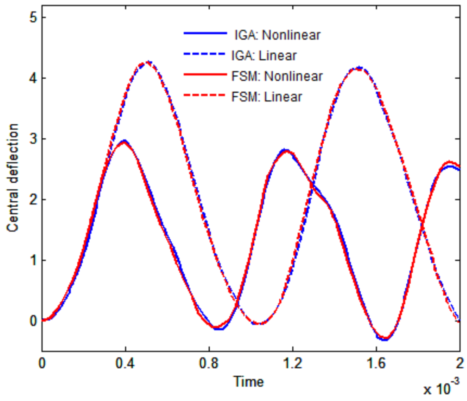

Fig. 3 Normalized central defections of the plate under step uniform load

3.2. Nonlinear analysis

3.2.1. An orthotropic plate

In this section, a SSSS square plate under a uniform loading of q_0 = 1 MPa with an aim to verify the accuracy of the present method for geometrically nonlinear transient analysis is studied. Material properties and the geometry are considered as follows: E_1 = 525 GPa, E_2 = 21 GPa, G_{12} = G_{23} = G_{13} = 10.5 GPa, v = 0.25, ρ = 800 kg/m^3, L = 250 mm, thickness h = 5 mm. Figure 3 shows the normalized central deflection, $\overline{w} = w / h$, of the plate. It can be seen that deflection responses of present method match well with those of finite strip method (FSM) [17].

3.2.2. Nonlinear control

We now consider a plate [*pie*/-45/45]$_s$ under step load. Figure 4 shows nonlinear transient vibrations of the central point of the plate under a closed-loop control. We observe that the response with control is smaller than those without control, as expected.

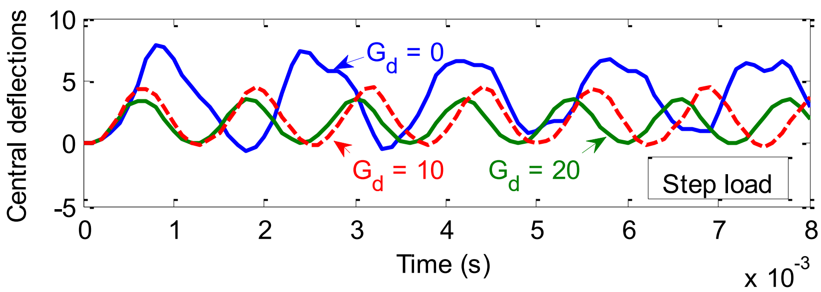

Fig. 4 Effect of the control gain on the nonlinear response of the piezoelectric composite plate.

4. CONCLUSIONS

This paper presents a simple and effective approach based on the combination of IGA and a generalized unconstrained approach for dynamic control and optimization of smart piezoelectric composite plates. The new function through the plate thickness for the UHSDT is introduced, which can achieve any desired degree of smoothness through the choice of the interpolation order and easily fulfills the C^1-continuity requirements for plate elements stemming from the HSDT. In analyses, the present approach would provide a reliable source of reference when calculating laminated composite plates with other methods.

ACKNOWLEDGMENTS

The first author would like to acknowledge the support from Erasmus Mundus Action 2, Lotus Unlimited Project.

5. REFERENCES

[1] Reddy JN (1997). Mechanics of laminated composite plates – Theory and Analysis, New York, CRC Press.

[2] Liu GR, Dai KY, Lim KM (2004). Static and vibration control of composite laminates integrated with piezoelectric sensors and actuators using the radial point interpolation method. Smart Materials and Structures, 13, 1438-1447.

[3] Torres DAF, Mendonca PdTR, Barcellos CSD (2011). Evaluation and verification of an HSDT-layerwise generalized finite element formulation for adaptive piezoelectric laminated plates. Computer Methods in Applied Mechanics and Engineering, 200, 675-691.

[4] Saravanos DA, Heyliger PR, Hopkins DA (1997). Layerwise mechanics and finite element for the dynamic analysis of piezoelectric composite plates. International Journal of Solids and Structures, 34, 359-378.

[5] Bailey T, Hubbard JE (1985). Distributed piezoelectric-polymer active control of a cantilever beam. Journal of Guidance Control and Dynamic, 8, 605–611.

[6] Shen IS (1995). Bending and torsional vibration control of composite beams through intelligent constrained-layer damping treatments. Smart Materials and Structures, 4, 340–355.

[7] Wang SY, Quek ST, Ang KK (2004). Dynamic stability analysis of finite element modeling of piezoelectric composite plates. International Journal of Solids and Structures, 41, 745-764.

[8] Phung-Van P, De Lorenzis L, Thai Chien H, Abdel-Wahab M, Nguyen-Xuan H (2015). Analysis of laminated composite plates integrated with piezoelectric sensors and actuators using higher-order shear deformation theory and isogeometric finite elements. Computational Materials Science, 96, 496-505.

[9] Phung-Van P, Nguyen-Thoi T, Luong-Van H, Lieu-Xuan Q (2014). Geometrically nonlinear analysis of functionally graded plates using a cell-based smoothed three-node plate element (CS-MIN3) based on the C 0-HSDT. Computer Methods in Applied Mechanics and Engineering 270, 15-36

[10] Phung-Van P, Abdel-Wahab M, Liew KM, Bordas SPA, Nguyen-Xuan H (2015). Isogeometric analysis of functionally graded carbon nanotube-reinforced composite plates using higher-order shear deformation theory. Composite Structures 123, 137-149.

[11] Phung-Van P, Nguyen-Thoi T, Luong-Van H, Thai-Hoang C, Nguyen-Xuan H (2014). A cell-based

smoothed discrete shear gap method (CS-FEM-DSG3) using layerwise deformation theory for dynamic response of composite plates resting on viscoelastic foundation. Computer Methods in Applied Mechanics and Engineering 272, 138-159.

[12] Phung-Van P, Thai-Hoang C, Nguyen-Thoi T, Nguyen-Xuan H (2014). Static and free vibration analyses of composite and sandwich plates by an edge-based smoothed discrete shear gap method (ES-DSG3) using triangular elements based on layerwise theory. Composites Part B: Engineering 60, 227-238.

[13] Phung-Van P, Lieu B Nguyen, Loc V Tran, Dinh TD, Chien H Thai, Bordas SPA, Abdel-Wahab M, Nguyen-Xuan H (2015). An efficient computational approach for control of nonlinear transient responses of smart piezoelectric composite plates. International Journal of Non-Linear Mechanics 76, 190-202.

[14] Leung AYT (1991). An unconstrained third-order plate theory. Composite Structures, 40(4), 871–875.

[15] Phung-Van P, Nguyen-Thoi T, Le-Dinh T, Nguyen-Xuan H (2013). Static and free vibration analyses and dynamic control of composite plates integrated with piezoelectric sensors and actuators by the cell-based smoothed discrete shear gap method (CS-FEM-DSG3). Smart Materials and Structures, 22, 095026.

[16] Cottrell JA, Hughes TJR, Bazilevs Y (2009). Isogeometric Analysis, Towards Integration of CAD and FEA, Wiley.

[17] Chen J, Dawe DJ, Wang S (2000). Nonlinear transient analysis of rectangular composite laminated plates. Composite Structures, 49, 129-139.